

IEEE TRANSACTIONS ON NANOTECHNOLOGY

A PUBLICATION OF THE IEEE NANOTECHNOLOGY COUNCIL

MARCH 2005

VOLUME 4

NUMBER 2

ITNECU

(ISSN 1536-125X)

PAPERS

Benchmarking Nanotechnology for High-Performance and Low-Power Logic Transistor Applications.	153
. <i>R. Chau, S. Datta, M. Doczy, B. Doyle, B. Jin, J. Kavalieros, A. Majumdar, M. Metz, and M. Radosavljevic</i>	
An Algorithm for Nanopipelining of RTD-Based Circuits and Architectures	159
. <i>P. Gupta and N. K. Jha</i>	
Carbon-Nanotube-Based Voltage-Mode Multiple-Valued Logic Design	168
. <i>A. Raychowdhury and K. Roy</i>	
Brownian Motion Model of Nanoparticle Considering Nonrigidity of Matter—A Systems Modeling Approach	180
. <i>N. N. Sharma and R. K. Mittal</i>	
ESA-Based In-Fiber Nanocavity for Hydrogen–Peroxide Detection.	187
. <i>I. Del Villar, I. R. Matías, F. J. Arregui, and R. O. Claus</i>	
Markov Chains and Probabilistic Computation—A General Framework for Multiplexed Nanoelectronic Systems.	194
. <i>Y. Qi, J. Gao, and J. A. B. Fortes</i>	
Spin Gain Transistor in Ferromagnetic Semiconductors—The Semiconductor Bloch-Equations Approach	206
. <i>D. E. Nikonov and G. I. Bourianoff</i>	
Nonphotolithographic Nanoscale Memory Density Prospects	215
. <i>A. DeHon, S. C. Goldstein, P. J. Kuekes, and P. Lincoln</i>	
High-Resolution Optical Imaging of Magnetic-Domain Structures	229
. <i>W. Dickson, S. Takahashi, R. Pollard, R. Atkinson, and A. V. Zayats</i>	
Structures and Electrical Properties of Ag–Tetracyanoquinodimethane Organometallic Nanowires	238
. <i>Z. Fan, X. Mo, C. Lou, Y. Yao, D. Wang, G. Chen, and J. G. Lu</i>	
SOI Single-Electron Transistor With Low <i>RC</i> Delay for Logic Cells and SET/FET Hybrid ICs.	242
. <i>K.-S. Park, S.-J. Kim, I.-B. Baek, W.-H. Lee, J.-S. Kang, Y.-B. Jo, S. D. Lee, C.-K. Lee, J.-B. Choi, J.-H. Kim, K.-H. Park, W.-J. Cho, M.-G. Jang, and S.-J. Lee</i>	
Crossbar Demultiplexers for Nanoelectronics Based on <i>n</i> -Hot Codes.	249
. <i>G. S. Snider and W. Robinett</i>	
Nanoscale Impedance Microscopy—A Characterization Tool for Nanoelectronic Devices and Circuits	255
. <i>L. S. C. Pingree, E. F. Martin, K. R. Shull, and M. C. Hersam</i>	
A New Dual-Material Double-Gate (DMDG) Nanoscale SOI MOSFET—Two-Dimensional Analytical Modeling and Simulation.	260
. <i>G. V. Reddy and M. J. Kumar</i>	
Periodically Structured Glancing Angle Deposition Thin Films	269
. <i>M. O. Jensen and M. J. Brett</i>	
Properties of Functionalized Redox-Active Monolayers on Thin Silicon Dioxide—A Study of the Dependence of Retention Time on Oxide Thickness	278
. <i>G. Mathur, S. Gowda, Q. Li, S. Surthi, Q. Zhao, and V. Misra</i>	
Modeling Hysteresis Phenomena in Nanotube Field-Effect Transistors	284
. <i>A. Robert-Peillard and S. V. Rotkin</i>	
Isolated Carbon Nanotubes as High-Impedance Transmission Lines for Microwave Through Terahertz Frequencies	289
. <i>M. J. Hagmann</i>	

BRIEF PAPERS

Size Dependence of Carrier Recombination Efficiency in GaN Quantum Dots	297
. <i>A. Neogi, H. Everitt, H. Morkoç, T. Kuroda, and A. Tackeuchi</i>	

Modeling Hysteresis Phenomena in Nanotube Field-Effect Transistors

Arnaud Robert-Peillard and Slava V. Rotkin, *Member, IEEE*

Abstract—A model is developed to explain a hysteresis observed experimentally in nanotube field-effect transistors. The model explains the hysteresis through trapping of electrons in an oxide layer. The Fowler–Nordheim tunneling mechanism is held responsible for the electron injection. The influence of different parameters such as the sweeping rate or the range of the gate voltage on the hysteresis is studied and compared with experimental results.

Index Terms—Electrostatics of one-dimensional (1-D) systems, field-effect transistors (FETs), hysteresis, nanotechnology, nanotube (NT) nonvolatile memory, NT transistors, tunneling.

I. INTRODUCTION

ONE promising direction for the transistors of the future involves “molecular electronics” in which the active part of the device is composed of a single molecule or a few molecules. One type of molecular electronic devices is based on carbon nanotubes (NTs). Their small diameters and their unique physical, chemical, and electronic properties may permit scaling beyond the limits of Si MOSFETs. NTs can be used to design nanotube field effect transistors (NT FETs) [1] with characteristics theoretically quite similar to MOSFETs. Experimental results displaying the ability to use these NT FETs as nonvolatile memory elements operating at the few-electron level have already been published [2]–[4]. The shift of the threshold voltage for gate voltage V_G increase and decrease, i.e., a hysteresis in the current/voltage curves has been observed and can be translated into memory effects.

The hysteresis is usually explained by a charge injection from the NT into the oxide at large gate bias, where the charges are trapped until the polarity is reversed. We propose a simple model, which explains the main experimental findings about the hysteresis by deriving dependence of the hysteresis width on the voltage scan range V_G^{Max} when exceeding some characteristic voltage. The sweeping rate (SR) of V_G influences the magnitude of the hysteresis because of slow traps discharging on a scale of seconds.

Manuscript received June 8, 2004; revised October 13, 2004. This work was supported by the Office of Naval Research under Grant NO0014-98-1-0604, by the Army Research Office under Grant DAAG55-09-1-0306, and by the National Science Foundation under Grant EEC-0228390. The work of S. V. Rotkin was supported by the Department of Energy under Grant DE-FG02-01ER45932 and by the National Science Foundation under Grant ECS 04-03489.

A. Robert-Peillard is with the Beckman Institute for Advanced Science and Technology, University of Illinois at Urbana-Champaign, Urbana, IL 61801 USA.

S. V. Rotkin is with the Physics Department, Lehigh University, Bethlehem, PA 18015 USA (e-mail: rotkin@lehigh.edu).

Digital Object Identifier 10.1109/TNANO.2004.842053

We explore electronic tunneling as the main mechanism for stable nonvolatile memory applications. We are aware that another model has been invoked to explain the experimental data in [4]. A possible dependence of the hysteresis on the relative humidity of the ambient was shown. The traps may actually be located very close to the surface of the oxide (a few nanometers), and water molecules adsorbed on the surface can weaken some bonds in the first layers of the oxide, which influences the trapping process. Water could also mediate the transfer of charge to and from the traps.

The ambient temperature also has an influence on the shift of the threshold voltage [3]: at lower temperature, fewer electrons are injected into the oxide. There is no explicit dependence of the hysteresis on temperature in our presented model, although this dependence is possibly related to the activation energy of the traps. A dependence similar to the one observed in NT FETs with the hysteresis greatly reduced at both low temperature (20 K) and high temperature (500 K) has been explained for MOSFETs invoking the anomalous positive charge [5]–[8]. This effect is also based on a reversible exchange of charge with the channel via a tunnelling mechanism.

II. THEORETICAL MODEL

We consider the following geometry of the device: a carbon NT of radius R contacted to side electrodes, and lying on an SiO_2 layer of thickness R_G and dielectric constant ϵ separating the NT from a back gate. To calculate the electrostatic part of the problem, we use a model with full axial symmetry. It is known that a solution for planar geometry differs from the axial one near the contacts only. We assume translational invariance of the problem with uniform potential V_G created by the gate on the NT.

The shift of the threshold voltage is due to the injection and the trapping/detrapping of carriers in the SiO_2 at large V_G . Experimentally, a sweep to large positive values of V_G creates a positive shift in the threshold voltage [3], indicating injection of *electrons*. These trapped electrons create an additive term to the external potential seen by the NT charge carriers. The external potential on the NT can be expressed as the sum of V_G and the potential created by trapped charges in the oxide. In our model, it has three contributions, which are: 1) V_- (the potential created by some negative charges); 2) V_+ (the potential created by positive traps close to the surface of the oxide); and 3) V_e (the potential created by the injected electrons populating these traps). The total external potential reads as

$$\phi_{\text{ext}} = V_G - V_- + V_+ - V_e. \quad (1)$$

TABLE I
VALUES OF THE DIFFERENT CONSTANTS USED FOR THE
TRAPPING/DETRAPPING MODEL

σ [5]	a [9]	b [9]	N_T	V_-	R_G	R_T	R	ϵ
10^{-18}	2.10^6	230	2.10^{13}	10	500	3	1	2.5
cm^2	$\frac{\text{A}}{\text{MV}^2}$	$\frac{\text{MV}}{\text{cm}}$	cm^{-2}	V	nm	nm	nm	-

The electric field at the NT/SiO₂ interface can be written as

$$\mathcal{E} = \frac{\phi_{\text{ext}}}{\left(R \ln \left(\frac{R_G}{R}\right)\right)} \quad (2)$$

where R is the NT radius, R_G is the effective gate distance, as defined above, and \mathcal{E} constitutes $\simeq 1$ V/nm at $\phi_{\text{ext}} \simeq 8$ V using the values for R and R_G given in Table I. In fact, that strong field is due to the one-dimensional (1-D) shape of the channel of the NT FET. This makes an important difference with the case of a standard MOSFET. The electrons can be injected into the oxide at such high field and remain trapped until the polarity is reversed, which causes hysteresis in the current/voltage curve.

We consider the tunneling of electrons through a triangular potential barrier at the NT/SiO₂ interface via a *Fowler–Nordheim tunneling electron injection* (FN-TEI) mechanism. The FN current as a function of the electric field at the barrier is $J_{\text{FN}} = a * \mathcal{E}^2 \exp(-b/\mathcal{E})$.

Using (2), we can redefine the constants a and b to write

$$J_{\text{FN}} = A * \phi_{\text{ext}}^2 \exp\left(\frac{-B}{\phi_{\text{ext}}}\right). \quad (3)$$

Substituting typical values for a and b for the FN tunneling in MOS devices, we calculate A and B . The kinetics law for the trapping of the electrons, a first-order differential equation for n [8], is used to calculate the rate of the trapping

$$\frac{dn}{dt} = \frac{J\sigma}{e}(N_T - n) \quad (4)$$

where N_T is the trap density, σ is the trapping cross section of the trapping centers, J is the tunneling current density, and n is the filled trap density (empty traps are assumed to be positive and become neutral when an electron is trapped). The rate of the detrapping process, which corresponds to the hole injection and further recombination with trapped electrons, at the reverse polarity, is given by

$$\frac{dn}{dt} = -\frac{J\beta}{e}n. \quad (5)$$

The constants A and B in this equation are slightly different as compared to the previous one, as the potential barrier for the holes is higher than for the electrons. We assume that σ and β have the same value and are field independent. To analytically calculate the potential created by the trapped charge density, we need to make several assumptions.

We approximate a trap density around the tube channel by the cylindrical volume with a thickness δ . Furthermore, we substitute a two-dimensional (2-D) charge distribution at the cylindrical surface instead of taking the volume integral over a bulk distribution n_{3D} . We then introduce an effective surface charge

density $n_T(\text{cm}^{-2}) = n_{3D} * \delta$ and an effective distance R_T to reflect the electric potential inside the oxide. R_T is chosen 3 nm, as experimental papers suggest that the injected electrons are trapped very close to the NT surface (the final result depends on the exact value of R_T only logarithmically though, it influences our choice of n_T). Their potential can then be calculated analytically as follows:

$$V_e = \frac{2\pi R_T n_T}{C_T} \quad (6)$$

where $C_T = 4\pi\epsilon_0\epsilon/(2\ln(R_G/R_T))$ is the trap capacitance. $\epsilon = [1 + \epsilon_{\text{SiO}_2}]/2$ is the effective dielectric constant of the oxide.

One substitutes the 2-D positive trap density N_T , assumed uniformly distributed, into (6) and calculate the potential of the positive traps V_+ in a similar way: $V_+ = 2\pi R_T N_T / C_T$. N_T should be high enough to match the experimental width of the hysteresis ($N_T \sim 10^{13} \text{ cm}^{-2}$). This high value may be explained in terms of water contamination at the open surface of the oxide, which increases the density of traps just beneath it. The last term in (1) is due to a potential of unspecified negative charges in the oxide V_- , which are not populated/depopulated, and it is a fitting parameter of the model to be discussed later.

Table I summarizes the values chosen for the variables defined in this paper.

III. RESULTS AND DISCUSSION

A full cycle of V_G starts at low positive ϕ_{ext} . The electric field \mathcal{E} given by (2) is small and there is no injection of electrons in the oxide. Thus, V_e is constant and ϕ_{ext} is linear in V_G . As we increase V_G , ϕ_{ext} and \mathcal{E} both increase, and so does the injection of electrons according to (3). Electrons start to fill the oxide traps, and V_e increases. For larger V_G , the increase in V_G is compensated by the increase in V_e . ϕ_{ext} and \mathcal{E} then become constant and independent of V_G . The gate voltage is large enough to provide enough electron injection, completely compensating increasing V_G as long as there are empty traps available near the NT. (The same happens for the large negative gate voltage.) This corroborates with the experimental fact [3] that the threshold voltage shift is equal to the increase in V_G at the large V_G , the slow sweep and room temperature.

We model the influence of two model parameters: the SR and the range of the gate voltage ($-V_G^{\text{Max}}, V_G^{\text{Max}}$) on the hysteresis H , which is just the shift of the external potential over a full cycle of V_G due to the injection of carriers at the large V_G (in all figures presented in this paper, H is represented for $V_G^{\text{Max}} = 10$ V and SR = 1 V/s).

Figs. 1 and 2 summarize the results of the modeling. We plot the external potential versus the gate voltage for different V_G^{Max} and SR. As expected, H increases linearly with the increase of V_G^{Max} for large enough V_G^{Max} . H will saturate at some value depending, of course, on the density of available traps N_T (around 22 V for our choice of parameters).

The SR also has an influence on the width of the hysteresis. It is obvious that the slower V_G is swept, the larger the density of injected electrons. Experimentally, substantial dependence of the width of the hysteresis on the SR has been observed [4]. The results of our model are presented in Fig. 2.

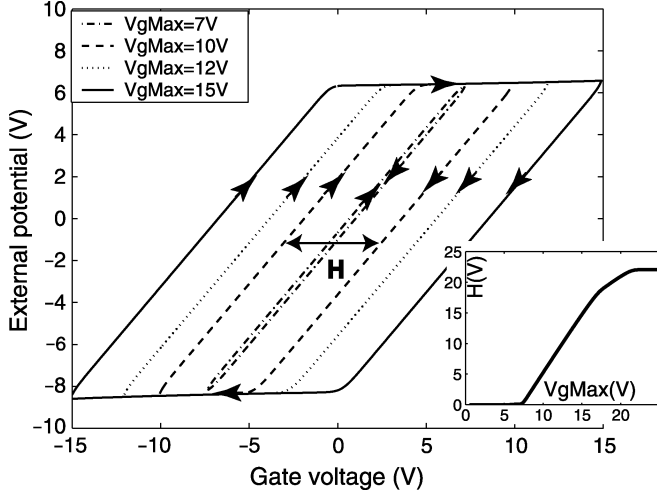


Fig. 1. Threshold voltage versus V_G calculated over a full cycle of V_G for different gate voltage ranges. $SR = 1$ V/s. Inset: width of the hysteresis as a function of V_G^{Max} .

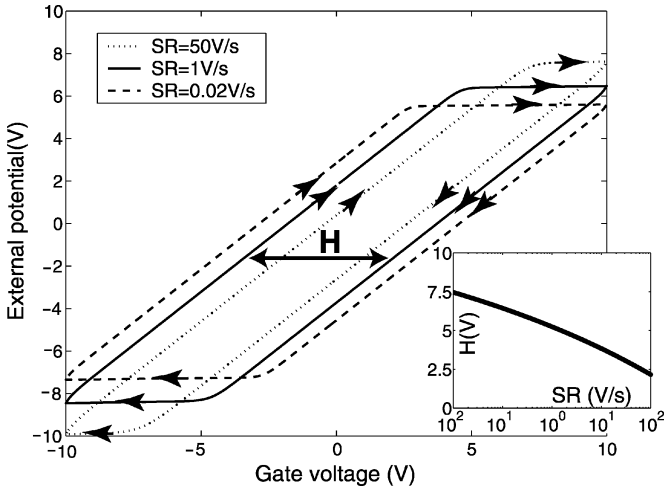


Fig. 2. Threshold voltage versus V_G calculated over a full cycle of V_G for different SR. $V_G^{\text{Max}} = 10$ V. Inset: semilog plot of the width of the hysteresis as a function of SR.

In this paper, we assume that the transport is diffusive. Approximation of the diffusion transport is usually good for semiconducting NTs longer than $1 \mu\text{m}$. The tube considered here is $5\text{-}\mu\text{m}$ long, as in [2], [3]. It has been discussed [10] that the NT total resistance is qualitatively the series resistance of a channel resistance and two contact resistances. Theoretical studies have shown that this is a good approximation for small drain voltages [11]. We have to note that our results are also applicable for calculation within a ballistic transport model, then (10) has to be substituted by a formula for a quantum-mechanical scattering coefficient. The charge density and self-consistent potential will be given by the same expressions.

We consider here an NT with p-type ohmic contact (no Schottky barrier to the valence band), which is usually the case experimentally with p-type contacts (metals with work functions larger than that of the NT, such as Au or Co).

We calculate the charge density and the potential on the tube following [12] for a cylindrical geometry. In our model, we calculate the effect of charges in the oxide on the external potential

using an approximation of translational invariance, which is accurate only far enough from the contacts, at the distances from them larger than the oxide thickness [12], which is much smaller than the length of the tube. Most of the tube can then effectively be described within our model.

The average total potential at the surface of the NT is given by $\phi = \phi_{\text{ext}} + \rho/C_G$, where ρ is the 1-D charge density along the NT and $C_G = 4\pi\epsilon_0\epsilon/(2\ln(R_G/R_T))$ is the geometrical capacitance to the (cylindrical) gate.

In equilibrium, the charge density is related to the position of the middle of the energy gap measured from the Fermi level E_F , $\tilde{E}_0 = E_0 - E_F$

$$\rho = e \int \text{sign}(E)\nu(E)f\left([E - \tilde{E}_0]\text{sign}(E)\right) dE \quad (7)$$

where f is the Fermi distribution (calculated at room temperature) and ν is the density of states (DOS). We will neglect the effect of higher 1-D subbands, as our calculations show that, for the range of ϕ_{ext} obtained here, $|\tilde{E}_0| < 2 * \Delta$ (second subband edge). Here, Δ is half of the band gap given by $\Delta = \hbar v_F/(3R) \simeq 0.2$ eV for $R = 1$ nm and a Fermi velocity $v_F \simeq 8 \times 10^5$ m/s. The DOS ν of a semiconducting NT is then given by the following expression [12]:¹

$$\nu(E) = \frac{4}{\pi\hbar v_F} \frac{|E|\Theta(|E| - \Delta)}{\sqrt{E^2 - \Delta^2}}. \quad (8)$$

Finally, the position of the Fermi level relative to the middle of the energy gap shifts with the total potential

$$\tilde{E}_0 = -e\phi + \Delta W = \frac{-e\phi_{\text{ext}} - e\rho}{C_G} + \Delta W \quad (9)$$

where ΔW is related to the work-function difference between contact electrodes and NT; $\Delta W = \Delta$, in our case, as we have assumed the p-type ohmic contact. We solve (7) and (9) in a self-consistent way to get the charge density.

The drift-diffusion modeling of the transport, as in [13], is used for the calculation of the tube resistance due to diffusive scattering. The nonequilibrium charge is computed within the linearization approximation [13] and, in the limit of small V_D , the tube resistance is given by

$$R_{\text{diff}} = \frac{2}{e\mu} \int_0^{\frac{L}{2}} \frac{dy}{\Delta\rho_e(y)}. \quad (10)$$

We choose a mobility $\mu = 9000$ $\text{cm}^2/\text{V/s}$ [3]. The equilibrium charge density $\Delta\rho_e(y)$ is uniform in the most of the tube for a $5\text{-}\mu\text{m}$ -long tube. Thus, we have $R_{\text{diff}} \simeq L/(e\mu\rho)$, where ρ is our self-consistent charge density calculated above in the translational invariance approximation.

We cannot explicitly calculate the dependence of the contact resistance on ϕ_{ext} , as it would require solving the problem close to the contact, where the translational invariance approximation does not hold. However, it has been shown both experimentally [10] and theoretically [14] that, in the case of the p-type ohmic

¹Our calculations have shown that the band structure near the first subband edge is almost unchanged under the external perturbations applied here.

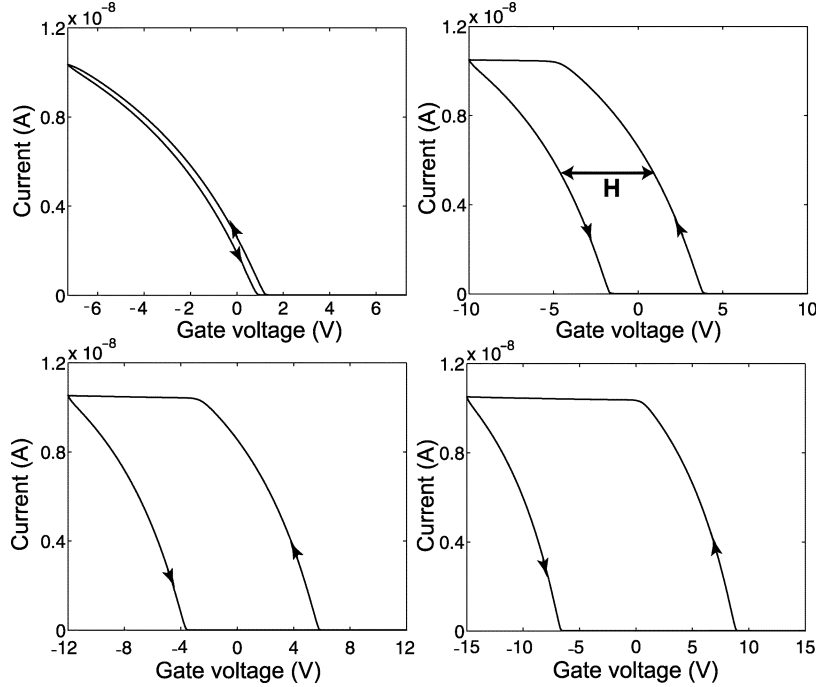


Fig. 3. Current versus V_G for different ranges of gate voltage; $SR = 1$ V/s. $V_D = 1$ mV. The NT is p-type.

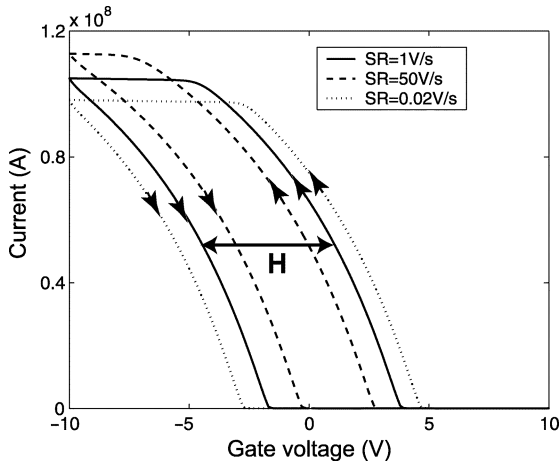


Fig. 4. Current versus V_G for different SR; $V_G^{\text{Max}} = 10$ V. $V_D = 1$ mV. The NT is p-type.

contact: 1) for p-type operation (Fermi level in the tube in the valence band at negative ϕ_{ext}), the contact resistance at each contact is small and relatively constant (we will use typical values of $30 \text{ k}\Omega$ [10], [14]) and 2) for n-type operation (Fermi level in the tube in the conduction band at positive ϕ_{ext}) and for relatively thick oxides (>100 nm, which is the case here), the contact resistance is very large (always in the megaohm region) due to the Schottky barrier in the conduction band for electrons, and then the device remains OFF even for very large positive ϕ_{ext} .

When the Fermi level in the tube is in the bandgap, the contact resistance changes abruptly, but if the tube resistance R_{diff} is very large, and the transport through the device is determined by R_{diff} , the value of the contact resistance in this region does not affect the current characteristics. The position of the Fermi level \tilde{E}_0 in the tube as a function of the external potential has been calculated in the self-consistent way according to (9).

Fig. 3 and 4 show the calculated currents.

The current is due to the p-type conduction. Close to the threshold voltages, the current increases almost linearly with $|V_G|$, as in the drift-diffusion model, and sublinearly further from the threshold when the contact resistance is comparable with R_{diff} . Furthermore, an injection of carriers into the oxide starts to occur at large enough negative ϕ_{ext} . Remember that, at that moment, ϕ_{ext} progressively saturates and becomes independent on V_G . Therefore, the current progressively saturates as well. For the n-type conduction region, the contact resistance keeps the device OFF, and the n-type conduction never shows up in our simulation.

IV. SUMMARY

We present a theoretical model for the hysteresis observed in NT FETs based on the tunneling and trapping of electrons in the oxide. Using rate equations for the trapping/detrapping process, we obtain the dependence of the width of the hysteresis on the SR and the range of the gate voltage, which match the experimental data well. Included in a semiclassical model of the transport in the NT, it provides the current-voltage characteristics in good agreement with experimental ones.

Here, we have studied only one mechanism for the hysteresis (based on the trapping of electrons in the oxide). The model gives the results consistent with most experimental observations. We are aware of the possibility of charge injection into the water adsorbed on the surface of the oxide, as it has also been suggested by several authors. The reaction involved still has to be elucidated, possibly being ionization or neutralization of some species under the high electric field. We have to notice that the possibility of the hysteresis being created by a diffusion of ions in the adsorbed water can be ruled out: a motion of positive ions in the electric field is toward the channel for positive V_G and, thus, always creates a negative shift in the gate voltage, where it has been observed to be positive.

ACKNOWLEDGMENT

The authors are indebted to Prof. K. Hess and Ms. Y. Li, both of the Beckman Institute, University of Illinois at Urbana-Champaign (UIUC), for valuable discussions.

REFERENCES

- [1] P. Avouris, "Molecular electronics with carbon nanotubes," *Acc. Chem. Res.*, vol. 35, pp. 1028–1036, 2002.
- [2] M. Radosavljevic, M. Freitag, K. Thadani, and A. Johnson, "Nonvolatile molecular memory elements based on ambipolar nanotube FETs," *Nano Lett.*, vol. 2, pp. 761–765, 2002.
- [3] M. Fuhrer, B. Kim, and T. Durkop, "High mobility nanotube transistor memory," *Nano Lett.*, vol. 2, pp. 755–760, 2002.
- [4] W. Kim, A. Javey, O. Vermesh, Q. Wang, and H. Dai, "Hysteresis caused by water molecules in carbon nanotube FETs," *Nano Lett.*, vol. 3, pp. 193–197, 2003.
- [5] Y. Roh, L. Trombetta, and J. Han, "Tunnel injection in silicon oxides prepared by rapid thermal oxidation," *J. Electrochem. Soc.*, vol. 142, pp. 1015–1020, 1995.
- [6] L. Trombetta, F. Feigl, and R. Zeto, "Positive charge generation in MOS capacitors," *J. Appl. Phys.*, vol. 69, pp. 2512–2516, 1991.
- [7] M. Fischetti, R. Gastaldi, F. Maggioni, and A. Modelli, "Positive charge effects on the flatband voltage shift during avalanche injection on Al–SiO₂–Si capacitors," *J. Appl. Phys.*, vol. 53, pp. 3129–3136, 1982.
- [8] A. El-Hdiy and D. Ziane, "Relaxation of positive charge during bidirectional electric stress on MOS capacitors," *J. Appl. Phys.*, vol. 86, pp. 6234–6238, 1999.
- [9] P. Samanta and C. Sarkar, "Analysis of positive charge trapping in SiO₂ of MOS capacitors during FN stress," *Solid State Electron.*, vol. 41, pp. 459–464, 1997.
- [10] Y. Yaish, J.-Y. Park, S. Rosenblatt, V. Sazonova, M. Brink, and P. L. McEuen, "Electrical nanoprobng of semiconducting carbon nanotubes using an atomic force microscope," *Phys. Rev. Lett.*, vol. 92, pp. 046 401-1–046 401-4, 2004.
- [11] S. Datta, *Electronic Transport in Mesoscopic Systems*. Cambridge, U.K.: Cambridge Univ. Press, 1998.
- [12] A. Odintsov and Y. Tokura, "Contact phenomena in carbon nanotubes," *J. Low Temp. Phys.*, vol. 118, pp. 509–515, 2000.
- [13] S. Rotkin, H. Ruda, and A. Shik, "Universal description of channel conductivity for nanotube and nanowire transistors," *Appl. Phys. Lett.*, vol. 83, pp. 1623–1626, 2003.

- [14] T. Nakanishi, A. Bachtold, and C. Dekker, "Transport through the interface between a semiconducting carbon nanotube and a metal electrode," *Phys. Rev. B, Condens. Matter*, vol. 66, pp. 073 307-1–073 307-4, 2002.



Arnaud Robert-Peillard received the B.A.Sc. degree in electrical engineering from the French Engineering School École Supérieure d'Electricité, Paris, France, in 2002, and the M.A.Sc. degree in electrical and computer engineering from the University of Illinois at Urbana-Champaign, in 2004.

He is currently with the Beckman Institute for Advanced Science and Technology, University of Illinois at Urbana-Champaign. His research is focused on the investigation of carbon NT transistors as nanoelectronic devices.



Slava V. Rotkin (M'02) received the M.Sc. degree (with honors) from St. Petersburg Electrical Engineering University, St. Petersburg, Russia, in 1994, and the Ph.D. degree in physics and mathematics from the Ioffe Institute, St. Petersburg, Russia, in 1997.

From 1994 to 1999, he was a Research Staff Fellow with the Ioffe Institute, Russian Academy of Sciences. From 1999 to 2003, he was a Beckman Fellow and, from 2003 to 2004, he was a Research Assistant Professor with the Beckman Institute for Advanced Science and Technology, University of Illinois at Urbana-Champaign. He is currently Frank J. Feigl Junior Faculty Scholar and Assistant Professor with the Physics Department, Lehigh University, Bethlehem, PA.

Dr. Rotkin was the recipient of numerous scientific awards, including the Arnold and Mabel Beckman Fellowship, the Royal Swedish Academy of Sciences Fellowship, the President and Government Grant for Young Scientists of Russia. He has authored over 70 publications concerning the theory of carbon-based systems, fundamentals of physics of NTs and nanowires, molecular and bio-complexes of NTs, and their device applications.